Output Feedback Control of Dissipative PDE Systems with Partial Sensor Information Based on Adaptive Model Reduction

Sivakumar Pitchaiah and Antonios Armaou
Dept. of Chemical Engineering, The Pennsylvania State University, University Park, PA 16802

DOI 10.1002/aic.13854
Published online June 15, 2012 in Wiley Online Library (wileyonlinelibrary.com).

We address the problem of control of spatially distributed processes in the presence of measurement constraints. Specifically, we assume the availability of sensors that measure part of the state spatial profile. The measurements are utilized for the derivation and on-demand update of reduced order models (ROM) based on an extension of the adaptive proper orthogonal decomposition (APOD) method using a snapshot reconstruction technique. The proposed Gappy-APOD methodology constructs locally accurate low-dimensional ROM thus resulting in a computationally efficient alternative to using a large-dimensional ROM with global validity. Based on the low-dimensional ROM and continuous measurements available from point sensors a Lyapunov-based static output feedback controller is subsequently designed. The proposed controller design method is illustrated on an unstable process modeled by the Kuramoto-Sivashinsky equation, when the designed controller successfully stabilizes the process even in the presence of model uncertainty. © 2012 American Institute of Chemical Engineers *AIChE J,* 59: 747–760, 2013
Keywords: distributed parameter systems, process control, adaptive model reduction, Kuramoto-Sivashinsky equation

Introduction

Over the last 20 years there has been increasing focus on analysis and control of processes that exhibit a spatial variations. The research activity in this area has been motivated by a wealth of industrially important processes (e.g., chemical vapor deposition and etching, catalytic reaction and polymerization processes), which exhibit significant spatial variations due to the presence of strong diffusive and convective mechanisms. Such distributed chemical processes can be mathematically described by parabolic partial differential equations (PDEs). The long-term dynamic behavior of parabolic PDEs is characterized by a finite-number of degrees of freedom.[1] This implies that the dynamic behavior of such chemical processes can be approximately described by finite-dimensional reduced order models (ROMs). As a result, some approaches design controllers for linear distributed processes using modal decomposition techniques retaining finite number of modes in the ROM[2] while others have focussed on balanced truncation techniques.[3] The impact of neglected modes (especially for hyperbolic PDEs) on the stability of designed controller was also analyzed.[4] In another approach, the concept of approximate inertial manifold[5,6] was used, leading to low-order ROMs that accurately describe parabolic PDEs. The resulting ROMs were subsequently used for designing nonlinear controllers.[7–9]

Correspondence concerning this article should be addressed to A. Armaou at armaou@engr.psu.edu.

However, the above approaches for the formulation of the reduced order model cannot be directly applied to systems which have nonlinear spatial differential operators or to problems defined over irregular spatial domains, since the eigenvalue-eigenfunction problem of the spatial operator for these systems cannot be analytically solved in general; it is, thus, difficult to derive the basis functions to expand the solution of the PDE systems. To overcome this limitation researchers have focused on data-driven methods, wherein data obtained from the system is used to obtain the required empirical basis functions. One such data-driven method, known as the method of snapshots was proposed by Sirovich,[10,11] based on Karhunen-Loève expansions (KLE) (also known as proper orthogonal decomposition (POD)). This method has been extensively utilized to ''empirically'' compute the basis functions using an ensemble of solution data obtained either through experimental observations or from detailed numerical simulations. It has also been profusely used in model reduction[12–14] and control[15–19] of distributed processes.

The main limitation of the above ROM construction approach using POD lies on the *ad-hoc* nature of the data-driven order reduction step, requiring that a representative ensemble of solutions exists for the process to be properly discretised. Since no well-defined methodology exists for generating such an ensemble the problem is usually addressed through extensive simulations, thus increasing the computational cost of the existing methods. We have recently presented an adaptive POD methodology (APOD) to alleviate the requirement for the representative ensemble by recursively updating the basis functions in a computationally

efficient way.[20,21] APOD was explicitly designed to efficiently utilize the snapshots obtained during closed-loop process evolution as opposed to all other KLE-based reduction approaches that are based on open-loop snapshots. These closed-loop snapshots and the resulting ROM account for the impact of the controller functional form on the process. The APOD methodology was subsequently used for the design for state and output feedback controllers. This approach, however, requires either continuous availability or periodic availability of full state measurement sensors. The availability of such full state measurements is usually restricted due to limited availability of sensors.

In this work, we relax the necessity for complete state measurements by requiring that periodically partial state measurements are available. These partial measurements are first reconstructed using gappy POD.[22] The reconstructed measurements are then utilized in APOD for updating the ROM. An output feedback controller is then designed based on continuous point measurements available from a restricted number of sensors. The proposed methodology is applied to address the problem of stabilization of a system modeled by Kuramoto-Sivashinsky equation.

Mathematical Formulation

We focus on designing output feedback controllers for highly dissipative PDEs (HDPDEs) (in the sense of Assumption 1) described by the following state-space system

$$\begin{gathered}\frac{\partial \bar{x}}{\partial t} = \mathcal{L}(\bar{x}) + b(z)u + f(\bar{x}) \\ y_c = \int_\Omega c(z)\bar{x}dz \\ y_m = \int_\Omega s_m(z)\bar{x}dz \\ y_r = s_r(z,t)\bar{x}\end{gathered} \tag{1}$$

subject to mixed-type boundary conditions

$$q\left(\bar{x}, \frac{d\bar{x}}{d\eta}, \ldots, \frac{d^{n_o-1}\bar{x}}{d\eta^{n_o-1}}\right) = 0 \text{ on } \Gamma \tag{2}$$

and the following initial condition

$$\bar{x}(z,0) = \bar{x}_0(z) \tag{3}$$

where $\bar{x}(z,t) \in \mathbb{R}^n$ denotes the vector of state variables, $z = [z_1, z_2, z_3] \in \Omega \subset \mathbb{R}^3$ is the vector of spatial coordinates, $u \in \mathbb{R}^l$ denotes the vector of manipulated inputs; Ω is the domain of definition of the process and Γ is its boundary. $y_c \in \mathbb{R}^l$ denotes the vector of controlled outputs and $y_m \in \mathbb{R}^p$ and y_r denote the vectors of measured outputs for control and state reconstruction respectively. $\mathcal{L}(\bar{x})$ is an n_0 order dissipative, possibly nonlinear, self-adjoint spatial differential operator which includes higher-order spatial derivatives, $f(\bar{x})$ is a nonlinear vector function, $q(\bar{x}, \frac{d\bar{x}}{d\eta}, \ldots, \frac{d^{n_o-1}\bar{x}}{d\eta^{n_o-1}})$ is a nonlinear vector function, which is assumed to be sufficiently smooth, $\left.\frac{d\bar{x}}{d\eta}\right|_\Gamma$ denotes the derivative in the direction perpendicular to the boundary and $\bar{x}_0(z)$ is the initial condition. $b(z) \in \mathbb{R}^l$ is a known matrix function of z of the form $[b_1(z)b_2(z)\cdots b_l(z)]$, where $b_i(z)$ describes how the i^{th} control action $u_i(t)$ is distributed in the spatial domain Ω, and $c(z)$ is a known vector function of z which is determined by the desired performance specifications in the domain Ω. We note that in the case of point actuation which influences the system at z_0 (i.e., $b_i(z)$ is equal to $\delta(z - z_0)$ where $\delta(\cdot)$ is the standard Dirac function), we approximate function $\delta(z - z_0)$ by a boxcar function with a finite value of $1/2\hat{\varepsilon}$ in the interval $[z_0 - \hat{\varepsilon}, z_0 + \hat{\varepsilon}]$ (where $\hat{\varepsilon}$ is a small positive real number) and zero elsewhere in the domain Ω.

An important component of this work is the sensors used. We assume the availability of two sets of measurements: (1) periodic (partial) snapshot measurements, y_r and (2) continuous measurements, y_m. The periodic measurements, y_r, are sampled at time instants $t_i = t_0 + \Delta i$, where $i = 0, 1, 2, \cdots$ and Δ is the sampling time. These measurements will be utilized during the formulation & update of the ROM for the above system of Eq. 1 and provide partial information of the state profile. The continuous measurements, y_m, are utilized in the design and operation of the designed output feedback controller. Note that y_r is a profile while y_m is a vector variable. $s_r(z, t)$ and $s_m(z)$ are the sensor shape functions corresponding to y_r and y_m, respectively. Without loss of generality, we consider the one-dimensional case; the sensor shape distribution for the periodic measurements, y_r, is expressed as a finite sum of boxcar functions

$$\begin{gathered}s_r(z,t_i) = \sum_{j=1}^{N_f} B(z; b_j(t_i), c_j(t_i)) \\ B(z; b_j(t_i), c_j(t_i)) = H(z - b_j(t_i)) - H(z - c_j(t_i))\end{gathered} \tag{4}$$

where $b_j(t_i)$ & $c_j(t_i)$ represent the boundaries of the boxcar function at time instant t_i, N_f is a finite number and $H(\cdot)$ is the standard Heaviside function. We assume that over time the whole spatial domain is "covered" by the sensor measurements, y_r. In contrast, for the continuous point measurements, y_m, we consider the most restrictive case wherein the corresponding sensor shape function is given by the dirac function $s_m(z) = \delta(z - z_i)$.

The PDE system of Eq. 1 can be recast as an infinite-dimensional system in the Hilbert space $\mathcal{H}(\Omega, \mathbb{R}^n)$, the space of n-dimensional vector functions defined on Ω that satisfy the boundary conditions in Eq. 2.

$$\mathcal{H} = \left\{ x \in L_2[\Omega, \mathbb{R}^n];\ q\left(x, \frac{dx}{d\eta}, \ldots, \frac{d^{n_o-1}x}{d\eta^{n_o-1}}\right) = 0 \text{ on } \Gamma \right\} \tag{5}$$

We define the inner product and norm in $\mathcal{H}$ as follows

$$(\phi_1, \phi_2) = \int_\Omega \phi_1^*(z)\phi_2(z)dz,\ ||\phi_1||_2 = (\phi_1, \phi_1)^{1/2} \tag{6}$$

where $\phi_1, \phi_2 \in \mathcal{H}[\Omega, \mathbb{R}^n]$. Defining the state function x on $\mathcal{H}$ as $x(t) = \bar{x}(z,t)$, $t > 0$, $z \in \Omega$, the operator $\mathcal{A}$ in $\mathcal{H}[\Omega, \mathbb{R}^n]$ as $\mathcal{A}(x) = \mathcal{L}(\bar{x})$, the input, controlled output and measured output operators as $\mathcal{B}u = bu$, $\mathcal{C}x = (c, x)$, $\mathcal{S}_m x = (s_m, x)$, $\mathcal{S}_r x = s_r x$, the system of Eqs. 1–3 acquires the following form in the Hilbert space, $\mathcal{H}$

$$\begin{gathered}\dot{x} = \mathcal{A}(x) + \mathcal{B}u + f(x),\ x(0) = x_0 \\ y_c = \mathcal{C}x,\ y_m = \mathcal{S}_m x,\ y_r = \mathcal{S}_r x\end{gathered} \tag{7}$$

where $f(x) = f(\bar{x}(z,t))$, $y_m \in \mathbb{R}^p$, $y_r \in \mathcal{H}[\Omega, \mathbb{R}^n]$, and $x_0 = \bar{x}_0(z)$.

Assumption 1. *The long-term dynamics of the PDE system of Eqs.* 1–3 *are finite-dimensional in a sense that the state x of the above system can be accurately described by a finite number of degrees of freedom. Thus, in principle, a finite number of appropriately chosen basis functions of* $\mathcal{H}$ *are sufficient to describe the long term behavior of x.*

Furthermore, the state modes x can be partitioned into a finite number of slow and possibly unstable modes and an infinite number of stable and fast modes and there is a time-scale separation between their dynamic behavior.

Remark 1 *Highly dissipative systems are exemplified by second-order parabolic PDE systems[9] that naturally arise in chemical engineering modeling. In general, physical phenomena that are described by HDPDEs include conduction during heat propagation, mass transfer under diffusion, instabilities in laminar flame fronts, phase dynamics in reaction-diffusion systems, and fluid film thickness during laminar flow on inclines. The proposed APOD methodology is applicable to processes described by HDPDEs,[20] such as vapor deposition and etching for LCD and microelectronics production, and the tin float bath process for flat glass production.*

Methodology

In this section, we will design the output feedback controllers for Eqs. 1–3 using the partial measurements and the APOD methodology. First, the available off-line (partial) process data in the representative ensemble is reconstructed using the gappy reconstruction procedure. These reconstructed off-line snapshots are first utilized to compute empirical basis functions. These basis functions are then used in Galerkins method to construct a reduced order model (ROM) for the above system. As the accuracy of a ROM constructed using the representative ensemble cannot be guaranteed globally, the design of controllers using such "global" ROM would be suspect. Consequently, we design the controller using a low-dimensional locally-valid ROM that has a small region validity (in the entire state space). The validity of this local ROM is extended (in a computationally efficient way) by periodically updating it using the reconstructed snapshots in APOD. The updated ROM along with continuous point measurements are later used to update the nonlinear static output feedback controllers and to stabilize the closed-loop system. In the next subsections we will first focus on the various individual steps involved in the procedure; at the end of this section we will combine the different steps and present the overall methodology.

Gappy reconstruction

The gappy reconstruction procedure[22] is utilized to reconstruct both the off-line snapshots $\{v_k\}_{k=1}^{N}$ and the online snapshots that become available during closed-loop process evolution. We first review this reconstruction procedure for the case of online snapshot reconstruction where the off-line snapshots are completely available followed by the situation wherein the off-line snapshots are incomplete, in the sense that certain part of the spatial domain solution is unavailable.

Complete Off-Line Snapshots. Let $\mathbf{V}_C = \{v_k\}_{k=1}^{N}$ be the collection of N snapshots, where v_k denotes the snapshot of the system state available at time t_k, i.e., $v_k = \bar{x}(z, t_k)$. Each snapshot, $\bar{x}(z, t_k)$, is the spatial profiles of the system states at a particular time instant, t_k. Let $\{\phi\}_{i=1}^{N}$ be the global basis functions computed by solving the following eigenvalue problem of the covariance matrix C_N[20] and using the method of snapshots[11] on the snapshot set $\mathbf{V}_C$. We assume that out of the N basis functions of C_N, w have the corresponding eigenvalues which capture ε percent of the energy of the ensemble, $\mathbf{V}_C$, i.e., $\sum_{i=1}^{w} \lambda_i / \sum_{i=1}^{N} \lambda_i \leq \frac{\varepsilon}{100}$ where λ_i is the ith eigenvalue of the covariance matrix C_N and ε is a user defined parameter. The incompleteness of the online data is usually characterized by mask functions. In a particular snapshot the associated mask function identifies the location of both the missing and the available data. In our application the sensor shape function defined in section plays the role of a mask function, i.e., $s(z, t_i) = 0$ if data is missing, else $s(z, t_i) = 1$.

Without loss of generality, let v_{N+1} be the online snapshot that needs to be reconstructed. Assuming that this snapshot can be characterized by the existing snapshot set, this is achieved by first computing an intermediate snapshot. The intermediate snapshot can be represented in terms of w basis functions ($w \leq N$) as follows

$$\tilde{v}_{N+1} \approx \sum_{i=1}^{w} \tilde{b}_i \phi_i \tag{8}$$

To compute the POD coefficients $\tilde{b}_i$, we minimize the following least-square criterion. The error that needs to be minimized is defined as $||v_{N+1} - \tilde{v}_{N+1}||_g^2$.

The "gappy" norm used in the above expression is defined based on the following inner product definition

$$(\phi, v_{N+1})_g = (\phi, s(z, t_{N+1}) v_{N+1}),\ ||v_{N+1}||_g = (v_{N+1}, v_{N+1})_g^{1/2} \tag{9}$$

where $s(z, t_{N+1})$ is the mask function for the $N + 1^{th}$ snapshot, v_{N+1}. Minimization of the above least-square criterion leads to the following set of linear equations

$$M\tilde{b} = f \tag{10}$$

where the $(i, j)^{th}$ element of the matrix M is given by

$$M_{ij} = (\phi_i, \phi_j)_g \tag{11}$$

and

$$f_i = (\phi_i, v_{N+1})_g \tag{12}$$

The intermediate snapshot $\tilde{v}_{N+1}$ is obtained by solving the linear system Eq. 10 for $\tilde{b}$ and substituting $\tilde{b}$ in Eq. 8. The snapshot, v_{N+1} is then reconstructed by replacing the missing data by the corresponding intermediate snapshot, i.e., $v_{N+1} = \tilde{v}_{N+1}$ if $s_r(z, t_{N+1}) = 0$.

$$v_{N+1}(z) = \begin{cases} v_{N+1}(z) & \text{if } s_r(z, t_k) \neq 0 \\ \tilde{v}_{N+1}(z) & \text{if } s_r(z, t_k) = 0 \end{cases} \tag{13}$$

Note that when we have a complete off-line ensemble of snapshots, the entire reconstruction is achieved at one step and is not iterative.

Incomplete Off-Line Snapshots. When the off-line snapshots are also not completely known, an iterative reconstruction procedure can be used to obtain the empirical basis functions. Let $\mathbf{V}_{IC} = \{v_k\}_{k=1}^{N}$, be the ensemble of incomplete snapshots along with an associated ensemble of masks $\{s(z, t_k)\}_{k=1}^{N}$. The masks can in general be generated randomly as considered in.[22,23] In this work, we confer a time-varying dependence to the masks such that over time the whole spatial domain is "covered" by the sensors. The iterative procedure consists of the following steps:

1. The first guess for the snapshot set is obtained by replacing the missing data in the off-line snapshots using smooth spline functions. Note that we avoid any bias due to the initial guess by carefully choosing the spline functions such that its average (over the regions where data is missing) matches the ensemble time average.

2. Use the standard POD technique to obtain the basis functions $\{\phi_k^l\}_{k=1}^{w^l}$ for the current iteration $\{l\}$.

3. Reconstruct all the snapshots in the snapshot set, $\mathbf{V}_{IC}$, by using w^l basis functions using the methodology for complete off-line snapshots described in the above section ($w^l \leq N$; choice of w^l depends on the desired accuracy). The intermediate snapshot set thus generated is represented by the snapshot set $\{\tilde{v}_k\}_{k=1}^{N}$.

4. The missing data in the snapshot set are now replaced with the reconstructed data i.e.

$$v_k^l(z) = \begin{cases} v_k^l(z) & \text{if } s_r(z,t_k) \neq 0 \\ \tilde{v}_k^l(z) & \text{if } s_r(z,t_k) = 0 \end{cases} \tag{14}$$

or

$$v_k^k(z) = \tilde{v}_k^l(z)(1 - s_r(z,t_k)) + v_k^l(z)s_r(z,t_k)$$

where $k = 1 \cdots N$.

5. The iterative procedure terminates once the eigenvalues computed by POD converge, i.e.

$$\max_{i=1\cdots w} |\lambda_i^{l+1} - \lambda_i^l| < \varepsilon_g \tag{15}$$

where λ_i^l is the ith eigenvalue of the covariance matrix C_N at the lth iteration and ε_g is a user defined convergence threshold. If the above criteria is not satisfied then we set $l = l + 1$ and go to step 2.

Remark 2 *Note that the convergence of the above reconstruction procedure depends on the quality of the initial guess. Consequently, during the initial iterations, the use of a large number of basis functions that capture a significant amount of energy of the snapshot set will result in significant errors in the reconstructed ensemble as the initial basis functions are inaccurate. To avoid this, during the initial iterations less energy is captured which subsequently increases. In the application section of this work for example, we used basis functions which capture 99% of energy for* ($l \leq 5$); *subsequently for* $l > 5$ *a higher energy of 99.99% was utilized for better accuracy. Converged results from the previous iterations are used during subsequent iterations. The above strategy significantly improves the convergence and accuracy of the iteration procedure; it also renders the methodology robust to initialization errors. A deeper discussion on the robustness of the off-line procedure to initialization errors can be found in.*[24]

Remark 3 *In step 1 of the above methodology, we use splines as an initial guess to replace the missing data as opposed to using a discontinuous time average.*[22,23] *The application of splines considerably improved the convergence of the above iterations as the initial basis functions are not discontinuous.*

Remark 4 *Note that in step* 4 *of the above procedure, we use the intermediate repaired snapshot to fill in the gaps of the missing data (see Eq.* 14). *As a result, the reconstructed snapshots will contain discontinuities at the boundaries between missing data and available data. These discontinuities arise due to the inherent errors associated with the gappy reconstruction procedure. Thus, when the gappy reconstruction procedure is utilized for design of online feedback controllers these discontinuities need to be monitored and even smoothened (appropriately to retain orthogonality) as they may potentially introduce large numerical errors when we compute spatial derivatives.*

Adaptive proper orthogonal decomposition

The gappy reconstruction procedure as presented in the previous section assumes that the snapshot to be reconstructed can be characterized by the existing snapshot set. This assumption in the realm of process control of distributed systems necessitates the *a priori* availability of a sufficiently large representative ensemble of PDE solution data in which all the possible spatial modes (especially including those that might appear in closed-loop evolution of the system in Eqs. 1–3) are excited and their long term behavior is also approximately captured. This is necessary to ensure that the resulting basis functions capture the global dynamics of the system and consequently gappy POD could be used, reliably, for the reconstruction of snapshots that may appear during the closed-loop process evolution.

The ROM computed using such representative ensemble of snapshots would be valid over the entire operational space, as the system passes through different regions of the state space during its closed-loop evolution. However, such ROMs tend to be of larger dimensionality and consequently implementing real-time feedback controllers using such ROMs is computationally demanding. In contrast, ROMs which are valid over a small operational region tend to be computationally efficient, however the validity of such models is limited to the region of the state space around which they are computed. To address both the validity and computational efficiency aspects of ROMs we now present an efficient algorithm called the adaptive proper orthogonal decomposition (APOD)[20,21] that allows for construction and recursive update of the ROM, as the new closed-loop measurements from the process become available. APOD allows us to use a locally valid ROM since it provides a computationally efficient way for updating the ROM on-demand and assures its validity over the current operational space. We now briefly present the prominent features of APOD. This methodology consists of the following three steps:

Initial Basis Construction. We initially use a collection of M ($M \leq N$) off-line data snapshots, $\{v_k\}_{k=1}^{M}$, to construct the initial local basis for Eqs. 1–3. Note that these M data snapshots cover a small operational space, consequently the basis computed using these snapshots may have a small region of validity. We first construct the covariance matrix C_M then solve the following eigenvalue-eigenvector problem[20]

$$C_M\psi = \lambda\psi$$

to compute M eigenvalues. We partition the eigenspace of the covariance matrix, C_M, into two subspaces; the dominant one containing the modes which capture at least ε percent of energy in the ensemble (denoted as $\mathbb{P}$) and the orthogonal complement to $\mathbb{P}$ containing the rest of the modes (denoted as $\mathbb{Q}$). By definition such a separation exists for dissipative processes and a finite number of modes belongs in $\mathbb{P}$, owing to the elliptic nature of the spatial differential operator[1] (assumption 1). Note that we define ε as the percentage energy of the ensemble captured by dominant basis functions.

We assume that out of M possible eigenvectors of C_M, $\tilde{w}$ ($\tilde{w} < w$) have the corresponding eigenvalues such that

$\sum_{i=1}^{\tilde{w}} \lambda_i / \sum_{i=1}^{M} \lambda_i \leq \frac{\varepsilon}{100}$; $\tilde{w}$ eigenmodes of C_M capture ε percent of energy in the ensemble. These eigenvectors are then used in the following equation

$$\phi_i(z) = \sum_{k=1}^{M} \psi_i^k v_k(z), \quad i = 1, ..., \tilde{w}$$

to compute $\tilde{w}$ basis functions; here ϕ_i represents the ith eigenfunction and ψ_i^k is the k^{th} element of the ith eigenvector of C_M. An orthonormal basis for the subspace $\mathbb{P}$ can be obtained as

$$Z = [\psi_1, \psi_2, ..., \psi_{\tilde{w}}], \quad Z \in \mathbb{R}^{M \times \tilde{w}} \tag{16}$$

where $\psi_1, \psi_2, ..., \psi_{\tilde{w}}$ denote the eigenvectors of C_M that correspond to the eigenvalues $\lambda_1, \lambda_2, ..., \lambda_{\tilde{w}}$. Note that the basis functions computed by these eigenvectors capture the dominant dynamics of the PDE system of Eqs. 1–3. The orthogonal projection operators $\mathbb{P}$ and $\mathbb{Q}$ onto subspaces $\mathbb{P}$ and $\mathbb{Q}$ can be computed as

$$P = ZZ^T, \quad Q = I - ZZ^T \tag{17}$$

where I denotes the identity matrix of dimension M.

Derivation of Reduced Order Model. In this section, we derive a locally valid ROM of the system of Eq. 7 using the above local basis functions. Using assumption 1, the Hilbert space $\mathcal{H}$ is partitioned into two subspaces $\mathcal{H}_s$ & $\mathcal{H}_f$, respectively. $\mathcal{H}_s$ includes the slow evolving modes whereas $\mathcal{H}_f$ includes fast evolving stable process modes. From the assumption $\mathcal{H}_f$ is an infinite-dimensional subspace, while $\mathcal{H}_s$ is a finite-dimensional one. Clearly, $\mathcal{H} = \mathcal{H}_s \oplus \mathcal{H}_f$. Defining orthogonal projection operator $\mathcal{Q}$ the state $x \in \mathcal{H}(\Omega)$ can be decomposed as $x_s = \mathcal{P}x \in \mathcal{H}_s$ and $x_f = \mathcal{Q}x \in \mathcal{H}_f$. The state x of the system of Eq. 7 now can be expressed as

$$x = x_s + x_f = \mathcal{P}x + \mathcal{Q}x \tag{18}$$

Applying projection operators $\mathcal{P}$ and $\mathcal{Q}$ to the system of Eq. 7 and using the above decomposition of x the system of Eq. 7 can be equivalently expressed as

$$\begin{gathered} \frac{dx_s}{dt} = \mathcal{A}_s(x_s, x_f) + \mathcal{B}_s u + f_s(x_s, x_f) \\ \frac{\partial x_f}{\partial t} = \mathcal{A}_f(x_s, x_f) + \mathcal{B}_f u + f_f(x_s, x_f) \\ y_c = \mathcal{C}x_s + \mathcal{C}x_f, y_m = \mathcal{S}_m x_s + \mathcal{S}_m x_f \\ x_s(0) = \mathcal{P}x(0) = \mathcal{P}x_0, x_f(0) = \mathcal{Q}x(0) = \mathcal{Q}x_0 \end{gathered} \tag{19}$$

where $\mathcal{A}_s = \mathcal{P}\mathcal{A}(x_s + x_f)$, $\mathcal{B}_s = \mathcal{P}\mathcal{B}$, $f_s = \mathcal{P}f$, $\mathcal{A}_f = \mathcal{Q}\mathcal{A}(x_s + x_f)$, $\mathcal{B}_f = \mathcal{Q}\mathcal{B}$, and $f_f = \mathcal{Q}f$ and the notation $\partial x_f / \partial t$ is used to denote that the state x_f belongs in an infinite-dimensional subspace ($\mathcal{H}_f$).

Using singular perturbation arguments for infinite-dimensional systems,[9] we neglect the infinite-dimensional fast and stable x_f subsystem in Eq. 19. The following $\tilde{w}$ -dimensional x_s subsystem is obtained

$$\begin{gathered} \frac{dx_s}{dt} = \mathcal{A}_s(x_s, 0) + \mathcal{B}_s u + f_s(x_s, 0) \\ y_{cs} = \mathcal{C}x_s, \; y_{ms} = \mathcal{S}_m x_s \\ x_f \equiv 0 \end{gathered} \tag{20}$$

where the subscript s in y_{cs} and y_{ms} indicates that these outputs are associated with the x_s subsystem. Under the assumptions already stated, the finite-dimensional system is an accurate approximation of the dominant dynamics of the infinite-dimensional system of Eq. 7.

Note that we use the basis functions, ϕ, computed in the previous section to define the subspaces $\mathcal{H}_s$ and $\mathcal{H}_f$, i.e., $\mathcal{H}_s = \text{span}\{\phi_1, \phi_2, ..., \phi_{\tilde{w}}\}$ and $\mathcal{H}_f = \mathcal{H} \setminus \mathcal{H}_s$. In order to ensure the validity of the decomposition the following assumption is made:

Assumption 2 *Subspace $\mathbb{P} \in \mathcal{H}$ defined as $\mathbb{P} = \text{span}\{\phi_1, \phi_2, ..., \phi_{\tilde{w}}\}$, where ϕ are basis functions identified via the APOD methodology using the covariance matrix C_M, appropriately captures the $\mathcal{H}_s$ subspace, i.e., $\mathcal{H}_s \subseteq \mathbb{P}$.*

As the basis functions, ϕ, have a small range of validity, the ROM (Eq. 20) computed using them may not remain valid during the course of closed-loop process evolution. To avoid this situation we periodically update the basis functions, ϕ, when necessary using APOD thus extending the ROMs validity over the current operational space.

Online Recursive Update of ROM. We update the locally valid ROM in Eq. 20, using periodic closed-loop snapshots y_r. Initially, we reconstruct these snapshots using the gappy reconstruction procedure in section. These reconstructed snapshots are then utilized to recursively update the orthonormal basis for the dominant subspace $\mathbb{P}$. This is achieved by either increasing or decreasing the size of the basis if required and by maintaining the accuracy of basis. The extra work required for the above process is small as long as the dimension of $\mathbb{P}$ is small. We then update the ROM in Eq. 24 using these updated basis functions. This step assures that during the closed-loop operation the ROM captures new trends that appear when the process traverses through previously unsampled regions in state space.

The algorithm outlined below computes an approximation to Z thus avoiding the need for resolving the eigenvalue-eigenvector problem of the covariance matrix, C_M. To simplify the algorithm we also assume that the dimensionality of the covariance matrix C_M remains constant. This is achieved by discarding the oldest snapshot from the ensemble as a new one is obtained. As a new snapshot from the process becomes available, the subspace $\mathbb{P}$ may change in the following three ways:

1. Increase in the dimensionality: During the course of process evolution one mode from $\mathbb{Q}$ may become dominant and, thus, would be necessary to be included in subspace $\mathbb{P}$ to capture the desired percentage of energy in the ensemble. This situation is ascertained by monitoring the contribution of the dominant eigenvalue of $c_q = QC_M\mathbb{Q}$, namely $\lambda_{\tilde{w}+1}$ towards the total energy of the ensemble, i.e., $\xi = \frac{\lambda_{\tilde{w}+1}}{\sum_{i=1}^{\tilde{w}+1} \lambda_i}$. If ξ increases to more than $(100 - \varepsilon)$ percent we append Z, the basis of subspace $\mathbb{P}$, with the corresponding eigenvector associated with $\lambda_{\tilde{w}+1}$.

2. Decrease in dimensionality: During the course of process evolution some of the eigenmodes of the subspace $\mathbb{P}$ may no longer be necessary to capture the desired ε percent of the energy. In this case the dimensionality of the basis Z is updated by decreasing it. To test this the following $\tilde{w} \times \tilde{w}$ matrix $H = Z^T C_M Z$ is introduced. If only $\hat{w}$, with $\hat{w} < \tilde{w}$, eigenvalues of H are dominant then the basis Z is updated and its dimension is simultaneously decreased.

3. Maintaining the accuracy: Even though the dimensionality of $\mathbb{P}$ remains unchanged, the basis Z is updated (whenever the current basis is not accurate) to maintain the

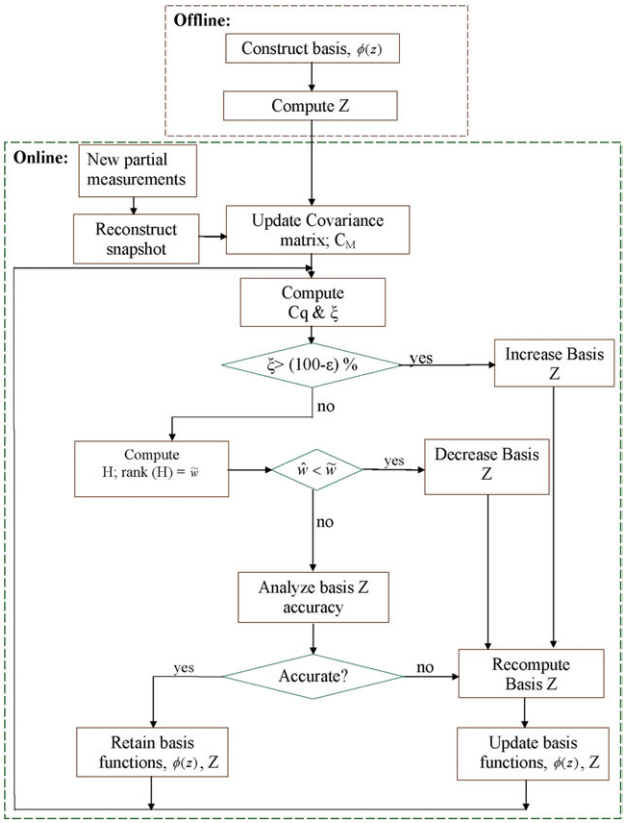

Figure 1. Flow chart of adaptive proper orthogonal decomposition methodology.

[Color figure can be viewed in the online issue, which is available at wileyonlinelibrary.com.]

accuracy of the basis. If after analyzing the accuracy of the current basis it is necessary to update the basis, the following one step power iteration $Z = \text{orth}\ (C_M Z)$ is executed.

A flow chart illustrating the above steps is presented in Figure 1. The detailed explanations for the above steps can be found elsewhere.[21] Based on the new values of Z, we then compute the revised basis functions $\phi_1, \phi_2, \ldots, \phi_{\tilde{w}}$ as a linear combination of the snapshots given by the following equation

$$\phi_i(z) = \sum_{k=1}^{M} \psi_i^k v_k(z), \quad i = 1, \ldots, \tilde{w} \tag{21}$$

where ψ_i^k denotes the $k^t h$ element of vector ψ_i. These updated basis functions are then utilized to update the ROM of Eq.20. In between the periodic updates of ROM, we assume that the updated ROM computed in Eq. 20 remains a valid representation of the original system in Eq. 7. The periodic updates guarantee that the assumption 2 remains valid for the duration of the closed-loop operation.

Complete closed-loop methodology

The complete closed-loop methodology, illustrating its different steps, is presented in Figure 2. We initially reconstruct the available (M) off-line data snapshots using the gappy reconstruction procedure off-line. These reconstructed snapshots are then used in the off-line step of APOD to construct an initial ROM. We then utilize the on-line step of APOD methodology (whose individual steps are presented in the previous subsection and illustrated in Figure 1) to periodically update the ROM using the closed-loop periodic (partial) snapshots, reconstructed online using gappy reconstruction procedure. The updated ROM along with continuous point measurements is then used to update the nonlinear static output feedback controllers and stabilize the closed loop system. The specific form and the stability aspects of the designed controller are discussed in the following section.

Nonlinear Static Output Feedback Control

In this section, we utilize the $\tilde{w}$ dimensional ROM of Eq. 20 to design nonlinear static output feedback controllers for the PDE system of the form given in Eqs. 1–3. In our previous results,[20,21] we designed state feedback and output feedback controllers for PDE systems based on continuous & periodic availability of full state measurements of the process. The availability of such full state measurements, even periodically, is usually restricted in practice due to high costs and reliability issues associated with these sensors. In this work we avoid this limitation by assuming the availability of partial snapshots, y_r, periodically. These periodic measurements are used for the state reconstruction and recursive update of ROM. We consider the synthesis of static output feedback controllers of the following form

$$u = \alpha(\tilde{x}_s) \tag{22}$$

where $\alpha(\cdot)$ is a smooth vector function and $\tilde{x}_s$ are the estimates of the states of the ROM Eq. 20. The above controller designed using the continuous point measurements, y_m, consists of two parts: (1) a Lyapunov- based state feedback controller[25] and (2) a state observer. Using the limited number of continuous point measurements, we design a static observer to estimate the states, $\tilde{x}_s$. The following assumption is needed in the design of the static observer.

Assumption 3 *The number of available point measurements, p, is equal to or greater than the dimension of subspace $\mathcal{H}_s$, i.e. $p \geq \tilde{w}$, and the inverse of the operator $\mathcal{S}_m$, $\mathcal{S}_m^{\perp}$, exists, so that $\tilde{x}_s = \mathcal{S}_m^{\perp} y_m$.*

The existence of inverse of matrix $\mathcal{S}_m$ depends on the location and shape of the measurement sensors; this amounts to properly choosing $s_m(z)$ in Eq. 1. Based on assumption 2, we can then use subspace $\mathbb{P}$ to approximate $\mathcal{S}_m^{\perp}$. When the finite-dimensional space, $\mathbb{P}$, is expressed using the empirical

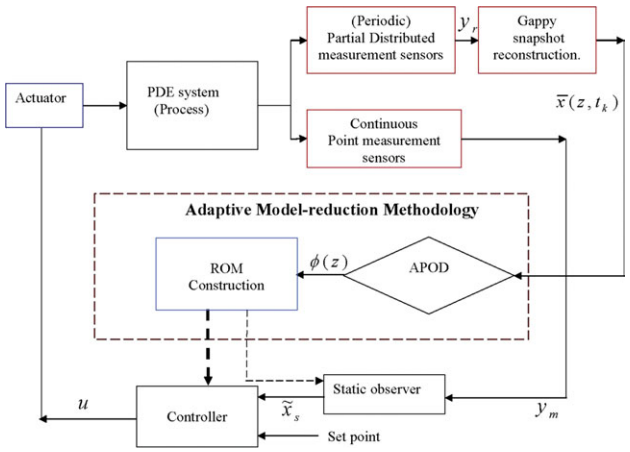

Figure 2. Block diagram of closed loop structure when using APOD.

[Color figure can be viewed in the online issue, which is available at wileyonlinelibrary.com.]

basis functions as basis functions the operator $\mathcal{S}_m^{\perp}$ becomes a matrix and is given by

$$\mathcal{S}_m^{\perp} = (\mathcal{S}_m^T \mathcal{S}_m)^{-1} \mathcal{S}_m^T \tag{23}$$

During the operation of the above controller, we use data alone from the point measurement sensors to identify the state. Consequently, the sensor shape distribution function, $s_m(z)$, is independent of time and is given by $s_{mi}(z) = \delta(z - z_i)$, where z_i is the location of ith sensor. The specific form and the stability aspects of the designed controller are discussed in the following lemma.

Lemma 1 *Consider the parabolic PDE system in Eq. 7, for which assumptions 1,2, and 3 hold. Also consider the nonlinear output feedback controller that is designed based on Eq. 20*

$$u = -k(\tilde{x}_s, c_0) L_{\mathcal{B}_s} V_{\tilde{w}}(\tilde{x}_s) \tag{24}$$

where

$$k(\tilde{x}_s, c_0) = \begin{pmatrix} c_o + \frac{L_{F_s} V_{\tilde{w}}(\tilde{x}_s) + \sqrt{(L_{F_s} V_{\tilde{w}}(\tilde{x}_s))^2 + (L_{\mathcal{B}_s} V_{\tilde{w}}(\tilde{x}_s))^4}}{(L_{\mathcal{B}_s} V_{\tilde{w}}(\tilde{x}_s))^2}, & L_{\mathcal{B}_s} V_{\tilde{w}}(\tilde{x}_s) \neq 0 \\ c_o & , L_{\mathcal{B}_s} V_{\tilde{w}}(\tilde{x}_s) = 0 \end{pmatrix}$$

$\tilde{x}_s = \mathcal{S}_m^{\perp} y_m$, $F_s = \mathcal{A}\tilde{x}_s + f_s(\tilde{x}_s, 0)$, $L_{F_s} V_{\tilde{w}} = \frac{\partial V_{\tilde{w}}}{\partial \tilde{x}_s} F_s$, $L_{\mathcal{B}_s} V_{\tilde{w}} = \frac{\partial V_{\tilde{w}}}{\partial \tilde{x}_s} \mathcal{B}_s$, $V_{\tilde{w}}(\tilde{x}_s(t_i)) = \frac{\zeta}{2} \tilde{x}_s(t_i)^T \tilde{x}_s(t_i)$, *where ζ is a periodically updated used-defined parameter. Then the controller in Eq. 24 asymptotically stabilizes the system in Eq. 7.*

Proof. Initially, we use Lyapunov arguments to prove that the closed-loop system of Eq. 20 is asymptotically stable. We then utilize multiple Lyapunov function analysis (from hybrid systems theory) to show that the systems remains stable during the periodic updates of the ROM. The above two parts are then synthesized together in part 3 to establish the asymptotic stability of the closed-loop system of Eq. 7.

Part-1: *(Closed loop stability of system of Eq. 7, between ROM revisions)*

Consider system in Eq. 20 of dimension $\tilde{w}$ for which assumption 3 holds. Evaluating the time-derivative of the Lyapunov function candidate

$$V_{\tilde{w}}(\tilde{x}_s(t)) = \frac{\zeta}{2} \tilde{x}_s(t)^T \tilde{x}_s(t) \tag{25}$$

along the trajectories of the system, we obtain

$$\dot{V}_{\tilde{w}} = L_{F_s} V_{\tilde{w}}(\tilde{x}_s(t)) + L_{\mathcal{B}_s} V_{\tilde{w}}(\tilde{x}_s(t)) u \tag{26}$$

where $\tilde{x}_s = \mathcal{S}_m^{\perp} y_m = \mathcal{S}_m^{\perp} \mathcal{S}_m (x_s + x_f) = x_s$ and ζ is an appropriately chosen positive number (discussed later). Substituting the controller in Eq. 24 into the above equation yields, after some algebraic manipulations.

$$\dot{V}_{\tilde{w}}(\tilde{x}_s(t)) = -c_0 (L_{\mathcal{B}_s} V_{\tilde{w}}(\tilde{x}_s(t)))^2 - \sqrt{(L_{F_s} V_{\tilde{w}}(\tilde{x}_s(t)))^2 + (L_{\mathcal{B}_s} V_{\tilde{w}}(\tilde{x}_s(t)))^4} \tag{27}$$

From the above equation, it is clear that $\dot{V}_{\tilde{w}}(\tilde{x}_s) < 0$. Therefore, given an initial condition $|\tilde{x}_s(0)| < \delta_s$, the closed-loop system of Eq. 20 is asymptotically stable under the controller of Eq. 24 [Theorem 4.1].[26]

Substituting the controller in Eq. 24 into Eq. 19, the closed-loop PDE system of Eq. 7 can be written in the following form

$$\begin{aligned} \frac{dx_s}{dt} &= \mathcal{A}_s(x_s, x_f) - \mathcal{B}_s k(\tilde{x}_s, c_0) L_{\mathcal{B}_s} V_{\tilde{w}}(\tilde{x}_s) + f_s(x_s, x_f) \\ \frac{\partial x_f}{\partial t} &= \mathcal{A}_f(x_s, x_f) - \mathcal{B}_f k(\tilde{x}_s, c_0) L_{\mathcal{B}_s} V_{\tilde{w}}(\tilde{x}_s) + f_f(x_s, x_f) \end{aligned} \tag{28}$$

Using assumption 1 the above system can be expressed in the following singular-perturbation form

$$\begin{aligned} \frac{dx_s}{dt} &= \mathcal{A}_s(x_s, x_f) - \mathcal{B}_s k(\tilde{x}_s, c_0) L_{\mathcal{B}_s} V_{\tilde{w}}(\tilde{x}_s) + f_s(x_s, x_f) \\ \varepsilon_s \frac{\partial x_f}{\partial t} &= \varepsilon_s \mathcal{A}_f(x_s, x_f) + \varepsilon_s f_f^*(x_s, x_f) \end{aligned} \tag{29}$$

where ε_s is a small number quantifying the separation between the dominant and nondominant eigenmodes of the spatial operator and f^* is defined as $f_f^*(x_s, x_f) = -\mathcal{B}_f k(\tilde{x}_s, c_0) L_{\mathcal{B}_s} V_{\tilde{w}}(\tilde{x}_s) + f_f(x_s, x_f)$. By the construction of the controller in Eq. 24 the term $f_f^*(x_s, x_f)$ does not contain terms of the form $O(1/\varepsilon_s)$.

Then, introducing the fast time-scale $\tau = t/\varepsilon_s$ and setting $\varepsilon_s = 0$, we obtain the following infinite-dimensional fast subsystem from the above equation.

$$\frac{\partial x_f}{\partial \tau} = \mathcal{A}_{f\varepsilon_s} x_f \tag{30}$$

where $\mathcal{A}_{f\varepsilon_s} = \varepsilon_s \mathcal{A}_f$. Note that $\mathcal{A}_{f\varepsilon_s}$ is of order $O(1)$ and the above system is locally exponentially stable by construction of system in Eq. 19 and assumption 2. Consequently after a period of time, t_f, during which the fast dynamics relax to zero, we may assume $x_f = 0$.[9] The closed-loop PDE system in Eq. 29 then reduces to the finite-dimensional slow system of Eq. 20, which was already proven to be asymptotically stable.

Part-2: *(Stability of hybrid system)*

In general, during the closed-loop process evolution, the periodic updates of ROM using APOD alters the underlying dominant subspace $\mathbb{P}$. As a result, the Lyapunov function $V_{\tilde{w}}$ and the controller in Eq. 24 are redesigned based on the updated ROM. Consequently, the stability aspects of the closed-loop system needs to be assessed using hybrid systems theory. To this end multiple Lyapunov functions are introduced of the same general form of 25. Under the assumption of finite number of ROM updates and finite time interval between ROM updates the following additional restriction on the Lyapunov functions guarantees the switched system to be Lyapunov stable [Theorem 3.2][27]

$$V_{\tilde{w}_1}(\tilde{x}_s(t_i)) < V_{\tilde{w}_2}(\tilde{x}_s(t_{i-1})) \tag{31}$$

where $i > 1$ and $V_{\tilde{w}_1}(\tilde{x}_s(t_i))$ corresponds to the value of the Lyapunov function at the beginning of the interval i for which the ROM is of dimension $\tilde{w}_1$.

Part-3: *(Combined analysis)*

The above condition is directly enforced in the APOD methodology during the ROM updates through the appropriate choice of ζ and ε and the periodic update of ζ value so that inequality Eq. 31 remains valid. This update can be automatically enforced. Thus, using the above condition under assumption 2 and the fact that the closed-loop system in Eq. 29 is asymptotically stable, we can conclude that the designed controller in Eq. 24 asymptotically stabilizes the system in Eq. 7. This concludes the proof.

Remark 5 *The presented APOD methodology can be very useful when optimization based controllers are considered (e.g., MPC). This is because an APOD based ROM implies that in the dynamic optimization formulation fewer ODE*

constraints will be present, while the accuracy of the reduced problem compared to the original one will remain largely unaffected. The design of such control structures is being currently investigated by the authors.

Remark 6 *The proposed control structure has a number of tuning variables, some that are implicit (and are explicitly connected with the ROM) and others that are explicit, such as* c_0 *and* ζ. *As discussed in the proof the value of* ζ *needs be chosen appropriately during dimensionality changes of the ROM. In general, higher values of* ζ *lead to more aggressive control action. A possible strategy is to automatically adjust* $\zeta = (\varepsilon/100)(\tilde{x}_s(t_i-1)^T\tilde{x}_s(t_i-1))/(\tilde{x}_s(t_i)^T\tilde{x}_s(t_i))$ *in order to retain an aggressive controller throughout the process operation. The strategy we used in the current work was to initialize* ζ *at value* 1 *and reevaluate it only when constraint 31 was violated based on the aforementioned formula.*

Kuramoto-Sivashinsky Equation

In this section, we illustrate the ability of the proposed output feedback controller in stabilizing the Kuramoto-Sivashinsky equation (KSE) using partial periodic measurements. KSE can adequately describe incipient instabilities arising in a variety of physio-chemical systems including falling liquid films,[28] unstable flame fronts, interfacial instabilities between two viscous fluids. Numerical studies[29] on the dynamics of KSE with periodic boundary conditions have revealed the existence of steady and periodic wave solutions, as well as chaotic behavior for very small values of v.

We consider the integrated form of the controlled Kuramoto-Sivashinsky equation

$$\frac{\partial x}{\partial t} = -v\frac{\partial^4 x}{\partial z^4} - \frac{\partial^2 x}{\partial z^2} - x\frac{\partial x}{\partial z} + \sum_{i=1}^{l} b_i u_i(t) \tag{32}$$

subject to the periodic boundary conditions

$$\frac{\partial^j x}{\partial z^j}(-\pi, t) = \frac{\partial^j x}{\partial z^j}(\pi, t), \quad j = 0, \ldots, 3 \tag{33}$$

and the initial condition

$$x(z, 0) = x_0(z) \tag{34}$$

where the state of the system x belongs to a Sobolev $\mathcal{W}4, 2$ space (i.e., $x \in \mathcal{H}([-\pi, \pi], \mathbb{R})$ of functions that are sufficiently smooth to be differentiable 4 times), z is the spatial coordinate, t is the time and $u_i(t)$ is the ith manipulated input. The spatial differential operator of system of Eq. 7, for this problem is of the form

$$\begin{aligned} &\mathcal{A}(x) = -v\frac{\partial^4 x}{\partial z^4} - \frac{\partial^2 x}{\partial z^2} - x\frac{\partial x}{\partial z} \\ &\left\{x \in \mathcal{H}([-\pi, \pi]; \mathbb{R}); \frac{\partial^j x}{\partial z^j}(-\pi) = \frac{\partial^j x}{\partial z^j}(\pi), j = 0, \ldots, 3\right\} \end{aligned} \tag{35}$$

where the length of the spatial domain is 2π and the diffusion parameter in Eq. 32 is set as $v = 0.25$. Six control actuators were assumed to be available at the following locations $L = [\pi/4, \pi/5, \pi/2, -\pi/2, -\pi/6, -\pi/4]$; the corresponding spatial distribution functions at these locations are $b_i(z) = \delta(z - L_i)$; $i = 1,\ldots,6$. Continuous point measurements were assumed to be available from 10 point measurement sensors placed uniformly across the domain of the process $(-\pi, \pi)$. The sensor shape distribution function, $s_m(z)$, for all time t, at these respective positions is $s_{mi}(z) = \delta(z - z_i)$; $i = 1, \ldots, 10$, where z_i is the location of ith sensor. In all the simulation runs, the following spatially nonuniform initial condition is considered

$$x_0 = 3\sin(z) - \cos(2z) - \sin(5z) + 2\cos(5z)$$

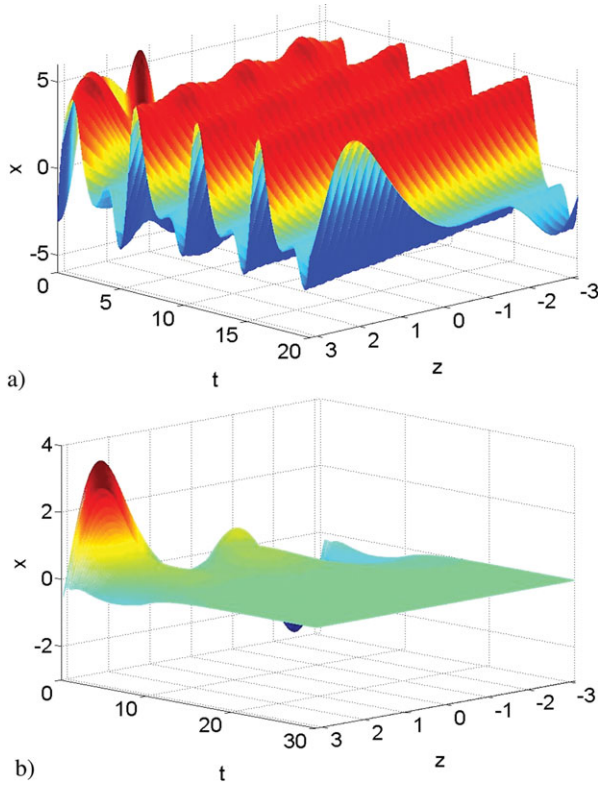

Figure 3. (a) Open-loop profile of the state of Eq. 32 with $v = 0.25$; (b) closed-loop profile of the state of Eq. 32.

[Color figure can be viewed in the online issue, which is available at wileyonlinelibrary.com.]

Figure 3, presents the traveling wave pattern observed in the open-loop evolution of KSE wherein we observe the formation of persistent waves. Thus, the control objective is set to stabilize the process at the spatially uniform steady state $x(z, t) = 0$.

Case 1: complete off-line snapshots

We assume that the snapshots that were collected off-line (to initially construct the basis functions) are complete without any missing spatial information. The online process measurements were however assumed to be available only from 10 point measurement sensors. The corresponding sensor shape distribution functions at these 10 locations are expressed as $s_m = s_r = \delta\ (z - z_i)$; $i = 1,\ldots,10$. We then utilized these point measurements in gappy reconstruction procedure for the online reconstruction of process states. As discussed in section, gappy reconstruction procedure assumes that the new snapshot to be reconstructed can be characterized by using the existing basis functions computed through off-line snapshots. To this end, we constructed an off-line representative ensemble of snapshots by exciting the system Eq. 32 using different variations in the input $u(t)$ profile.[12,30] Application of POD to this ensemble resulted in $w = 8$ global basis functions that captured 99% of the energy of the ensemble. These basis functions were further used to

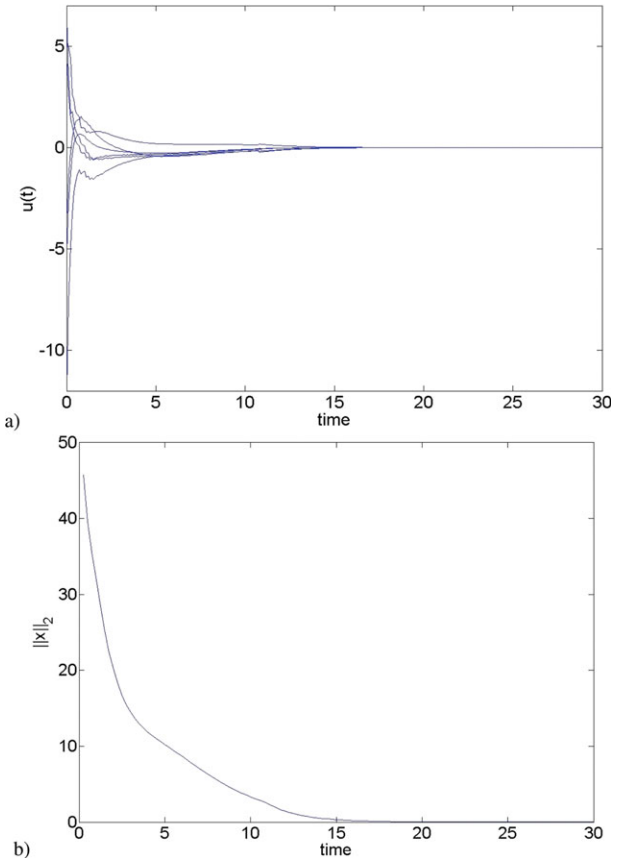

Figure 4. (a) Temporal profile of the control action, *u*(*t*). (b) Temporal profile of the Lyapunov function, *V*(*t*). ($\varepsilon = 0.99$).

[Color figure can be viewed in the online issue, which is available at wileyonlinelibrary.com.]

compute the global ROM (section). The computed global ROM captured the entire closed-loop process dynamics, thus ensuring an accurate online gappy reconstruction of process states.

However, the computed ROM tended to be of higher dimensionality; consequently the design of controller using such global ROM is computationally expensive. To demonstrate an alternative procedure, we used the computed global ROM only for online state reconstruction. In contrast, the controller was designed using a low-dimensional local ROM that was valid over a local operational region. Then, we periodically updated the local ROM using APOD, thus re-establishing ROM validity over the current operational space.

To design the controller, an initial ensemble of 100 open-loop snapshots ($M = 100$) was collected by simulating the process with $u(t) \equiv 0$ till $t = 2$. Application of APOD to this ensemble resulted in $\tilde{w} = 3$ basis functions that captured 99% of the energy of the ensemble. These basis functions were then used in the computation of the local ROM (Eq. 20) for the above process. Based on this ROM, an output feedback controller of Eq. 24 was subsequently designed, to achieve the desired control objective. We assume that partial closed-loop state information becomes available every $\delta t = 0.25$. The recursive check of the local ROM validity and consequently the task of online reconstruction of the snapshots was undertook at a period of every $\delta t = 0.25$. The parameter ζ in Eq. 25 was set to be $\zeta = 1$ initially. The percentage error for snapshot reconstruction was computed as

$$e_{\text{percent}} = \frac{||v_{N+1} - \tilde{v}_{N+1}||_2}{||v_{N+1}||_2} 100 \tag{36}$$

while the absolute error was computed as follows

$$e_{\text{absolute}} = ||v_{N+1} - \tilde{v}_{N+1}||_2 \tag{37}$$

where v_{N+1} is the online snapshot that needs to be reconstructed and $\tilde{v}_{N+1}$ is the gappy reconstructed snapshot (see Eq. 8).

Figure 3b presents the closed-loop evolution profile of KSE under the designed controller. The controller successfully stabilized the process at the desired operating point of $x(z, t) = 0$. The control action used for achieving this result is presented in Figure 4a. We observe that the control action is a smooth function of time which converges to zero at the end of the successful closed-loop process operation. Figure 4b presents the temporal profile of the Lyapunov function $V_{\tilde{w}}(t)$. As the designed controller successfully stabilizes the process the Lyapunov function converges uniformly to zero. Figure 5a presents both the percentage error and the absolute error in on-line state reconstruction from 10 point sensors using gappy reconstruction procedure. We note that both the

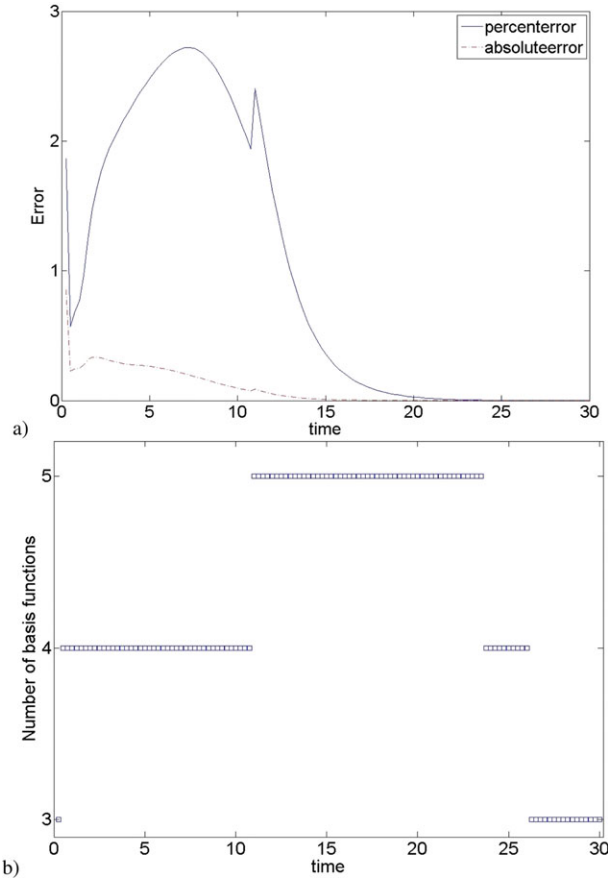

Figure 5. (a) Temporal profile of the state reconstruction error using gappy reconstruction; (b) temporal profile of dimensionality of the local ROM of Eq. 32 ($\varepsilon = 0.99$).

[Color figure can be viewed in the online issue, which is available at wileyonlinelibrary.com.]

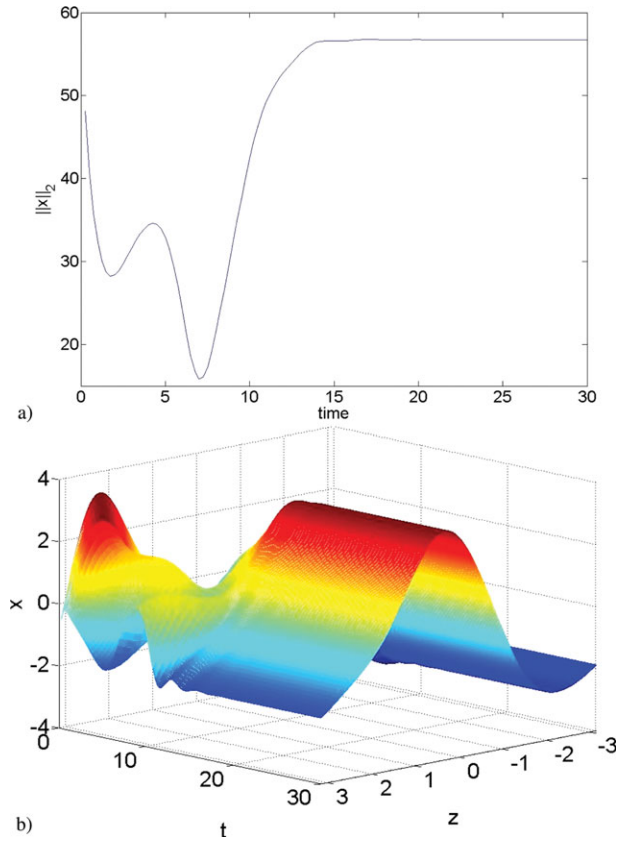

Figure 6. (a) L_2 norm of the closed-loop profile of Eq. 32 without APOD; (b) closed-loop profile of state of Eq. 32 without APOD ($\varepsilon = 0.99$).

[Color figure can be viewed in the online issue, which is available at wileyonlinelibrary.com.]

percentage error and the absolute error stay within 3% and reach zero as the control objective is achieved. Note that the spike in the percentage error observed at $t = 11$ corresponds to a small change in the absolute error and is due to a system response to an increase in the control action (Figure 4a) caused because the dimensionality of the ROM changes as determined by APOD.

The change in the dimensionality of the local ROM is presented in Figure 5b. Note that the dimensionality of a global ROM computed using POD remains at 8; in contrast, the dimensionality of a local ROM starts at 3 and increases to 5 for a brief time and then becomes 3 again. Using a local ROM considerably reduced the computational effort, while designing ROM based controllers that stabilized the process. This observed improvement will be more prominent during the implementation of APOD on a large scale process. We also note that it was not necessary to change the value of ζ, which remained constant at $\zeta = 1$ throughout the simulation.

To present the importance of APOD in updating the local ROM, we now switch off the APOD and implement the controller that was designed based on the local ROM with a corresponding dimensionality $\tilde{w} = 3$. As the validity of the local ROM was restricted to a small region of the operational space and the closed-loop process traversed through a different region of the state space, the local ROM failed to describe the process. The corresponding closed-loop profile L_2 norm and the state is presented in Figures 6a, b, respectively. It is evident that the controller failed to achieve the necessary control objective.

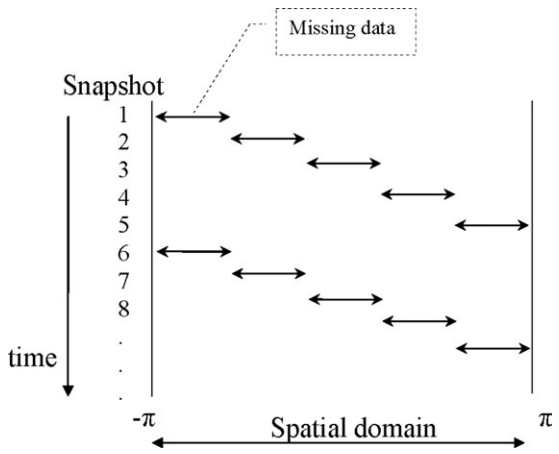

Figure 7. Pattern of missing data due to scheduling of sensors.

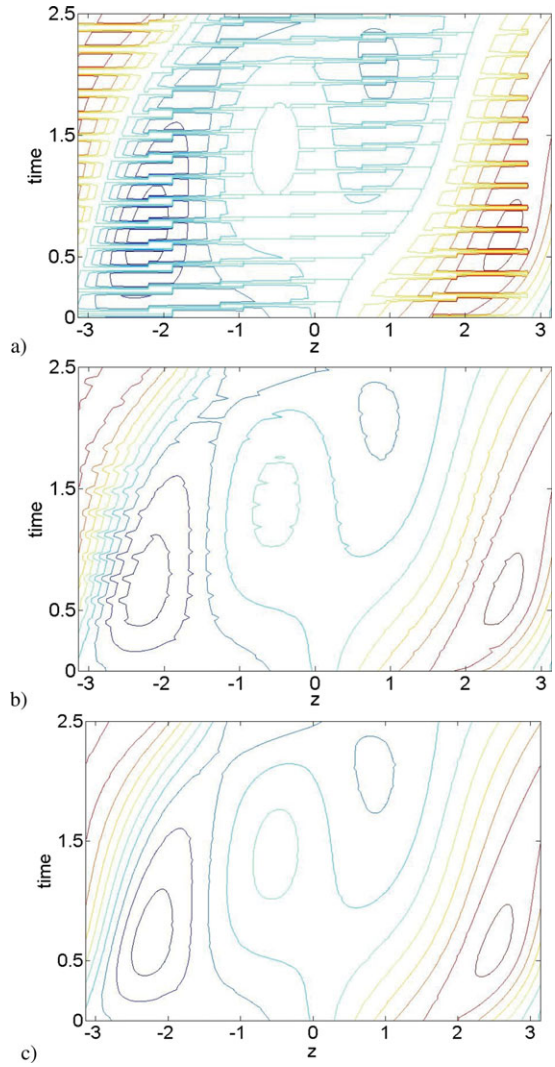

Figure 8. (a) Contour plot of the evolution of KSE from $t = 0$ to $t = 2.5$ with 20% data missing per snapshot; (b) contour plot after 1st iteration using gappy reconstruction procedure (c) Contour plot after 30th iteration.

[Color figure can be viewed in the online issue, which is available at wileyonlinelibrary.com.]

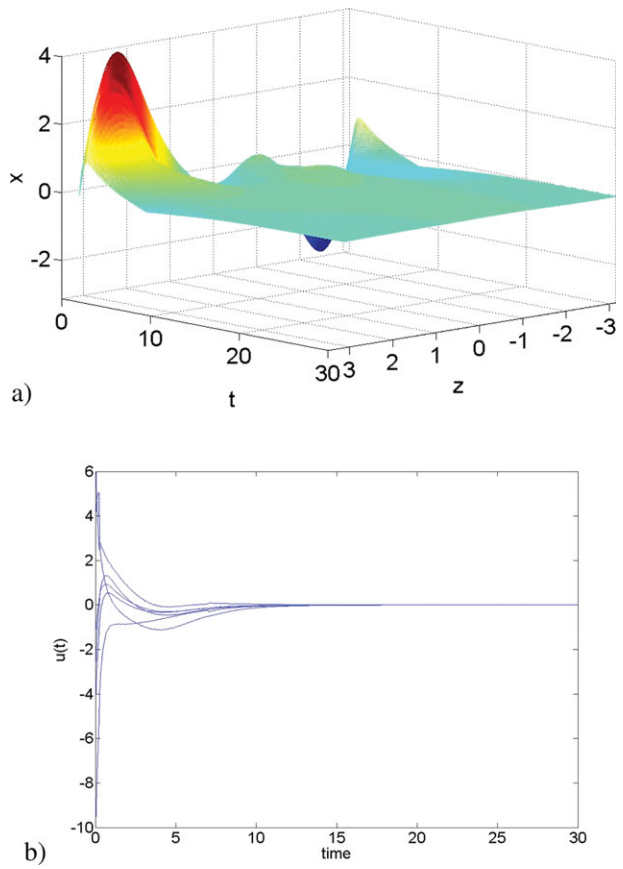

Figure 9. (a) Closed-loop profile of the state of Eq. 32; (b) temporal profile of the control actuation, $u(t)$ ($\varepsilon = 0.99$).

[Color figure can be viewed in the online issue, which is available at wileyonlinelibrary.com.]

Case 2: partial off-line snapshots

In case 2, we assume that the snapshots that were collected off-line (for construction of POD basis functions) were incomplete, i.e., there are regions where information was unavailable. A typical pattern used for the incomplete data is presented in Figure 7. Note that there was no particular spatial subregion of the domain that remained unobservable for all times. In the presented simulations, at any time instant 20% of the data in each snapshot was missing.

First we utilized the iterative gappy reconstruction procedure to "fill" in the incomplete data. The different stages involved in using this reconstruction procedure are presented in Figure 8a by using open-loop contour plots. Initially, we "replaced" the gaps in all the snapshots using a spline interpolation. Then we utilized this new ensemble as a first guess to construct an approximate POD basis. As discussed in remark 2, we note that a POD basis was constructed to capture 99% energy of the off-line ensemble during the initial iterations ($l < 5$) and for the rest of iterations an higher energy of 99.99% was used. Figure 8b presents the approximation of the ensemble at the end of the first iteration and Figure 8c presents the approximation of the ensemble at the end of the 30th iteration. We note that as we increase the number of iterations the ensemble matches close to the original ensemble with no missing data. We note that a similar reconstruction procedure was performed on the (global) ensemble.

After the reconstruction of the off-line ensemble, we followed the proposed procedure elucidated the methodology section. We initially derived the global ROM for the online reconstruction of snapshots and subsequently we derived a local ROM for the efficient design of online feedback controllers. As in the previous case, we collected an initial ensemble of 100 open-loop snapshots by simulating the process with $u(t) \equiv 0$ till $t = 2.5$ and utilized APOD to compute a ROM using a 99% energy criterion. A local ROM was then derived using these basis functions and was utilized to design an output feedback controller of Eq. 24, setting $\zeta = 1$ initially. The periodic update of local ROM and consequently the online reconstruction of the snapshot was pursued at a period of every $\delta t = 0.25$.

Figure 9a presents the closed-loop evolution profile of KSE. We note that the controller successfully stabilized the process at the desired operating point of $x(z, t) = 0$. The control action used for achieving this result is presented in Figure 9b. Similar to the previous case, we observe that the control action smoothly converges to zero at the end of closed-loop process operation. Figures 10a, b present the temporal profile of the L_2 norm of the system and the Lyapunov function $V_{\tilde{w}}(t)$, respectively. Both the L_2 norm and Lyapunov function converge uniformly to zero, even though there is a increase in the dimensionality of the ROM at $t \approx 8$, thus indicating the successful closed-loop operation.

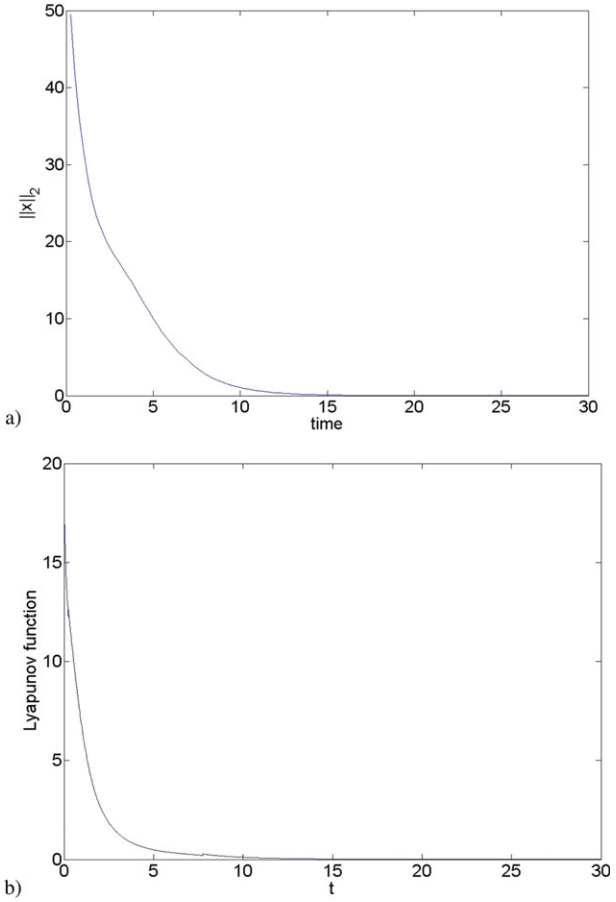

Figure 10. (a) L_2 norm of the closed-loop profile of Eq. 32; (b) temporal profile of the Lyapunov function, $V(t)$ ($\varepsilon = 0.99$).

[Color figure can be viewed in the online issue, which is available at wileyonlinelibrary.com.]

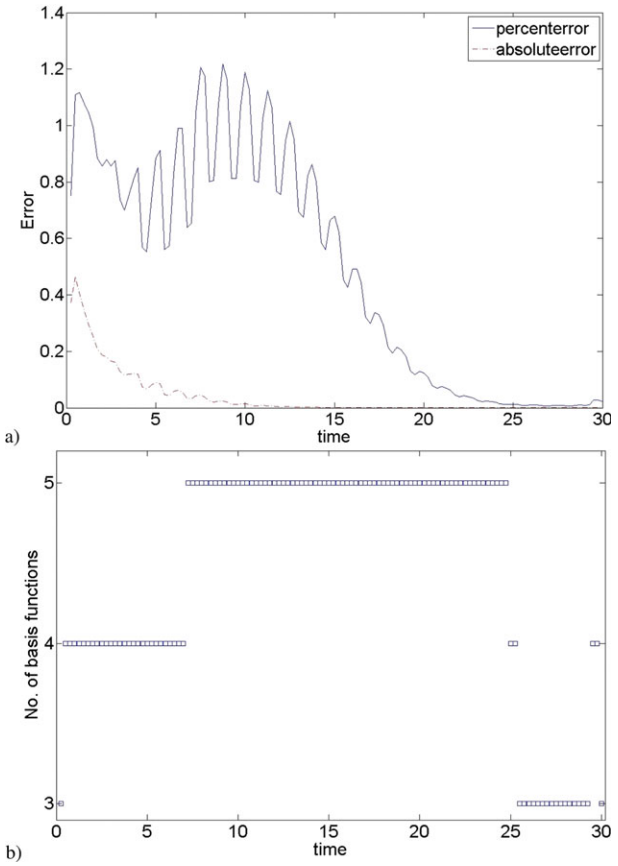

Figure 11. (a) Temporal profile of the state reconstruction error using gappy reconstruction; (b) temporal profile of dimensionality of the local ROM of Eq. 32 ($\varepsilon = 0.99$).

[Color figure can be viewed in the online issue, which is available at wileyonlinelibrary.com.]

Figure 11a presents both the percentage error and the absolute error in on-line state reconstruction from snapshots with 20% incomplete data. The oscillation observed in the percentage error is due to the discontinuities that arise as the boundary points between the missing data and available data changes as presented in Figure 7. We note that both the percentage error and the absolute error stay within 1.2%. The change in the dimensionality of the local ROM is presented in Figure 11b. The global ROM that would capture all the closed-loop process characteristics would require the dimensionality of 8 to capture 99% of the energy of the global ensemble. In contrast, the dimensionality of the local ROM started at $\bar{w} = 3$ and increased to 5 at $t \approx 8$ and then reduced to a dimensionality of 3 at the end of process operation. Thus, the use of local ROM significantly reduced the computational effort in the implementation of the online controller. We also note that it was not necessary to change the value of ζ, which remained constant at $\zeta = 1$ throughout the simulation.

To further illustrate the applicability of the methodology, we also investigated different values of the instability parameter ν. A graph presenting the order of the system for different values of the diffusion parameter (ν) is presented in Figure 12a and corresponding closed loop L_2 norm is presented in Figure 12b. For each of the different diffusion parameters used, the controller successfully stabilized the

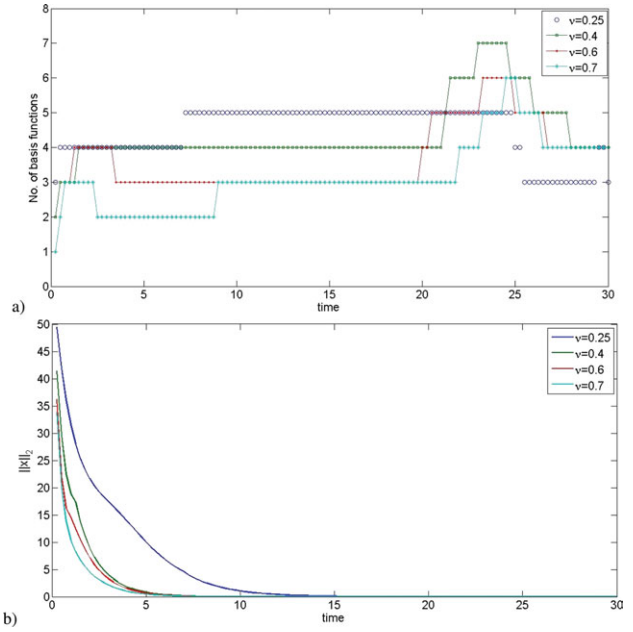

Figure 12. (a) Order of system for different instability parameters; (b) closed loop L_2 norm of the system for different instability parameters ($\varepsilon = 0.99$).

[Color figure can be viewed in the online issue, which is available at wileyonlinelibrary.com.]

system. This implies that the control design methodology is successful in designing controllers that stabilize the KSE independently of the process parameters.

An important question that may arise is how would Gappy APOD compare to standard APOD and if a significant computational cost is incurred. Figure 13 compares the computational effort of Gappy APOD as a function of time and it is compared to regular APOD (assuming full data availability). We observe that the additional burden due to gappy reconstruction is relatively small. This implies that the online Gappy reconstruction procedure is fast. Since we have previously shown the significant computational savings of APOD compared to recursively using standard POD,[20] we maintain that the computational burden of the proposed controller design remains small.

To test the effectiveness of the methodology under significant parametric uncertainty, we assumed a 40% uncertainty

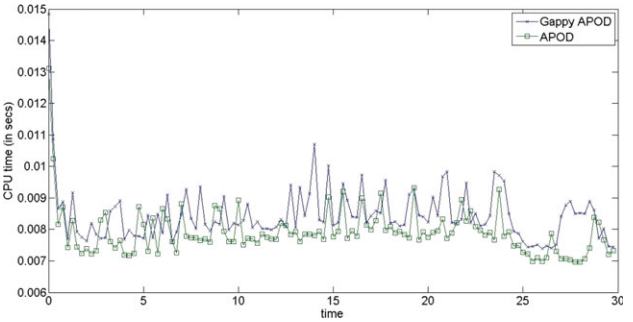

Figure 13. Computational effort of Gappy APOD and regular APOD as a function of time ($\varepsilon = 0.99$).

[Color figure can be viewed in the online issue, which is available at wileyonlinelibrary.com.]

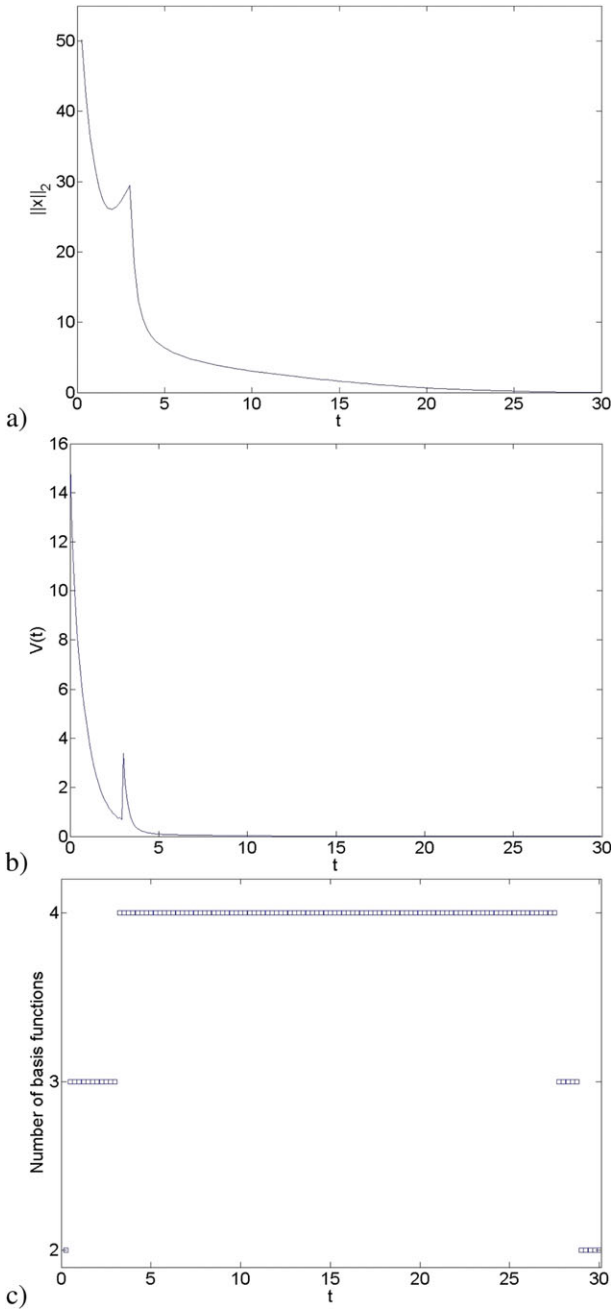

Figure 14. Closed-loop process evolution for small value of $\varepsilon = 0.9$ (a) L_2 norm of the closed-loop profile of Eq. 32; (b) temporal of the Lyapunov function, $V(t)$; (c) temporal profile of dimensionality of the local ROM of Eq. 32.

[Color figure can be viewed in the online issue, which is available at wileyonlinelibrary.com.]

in the diffusion parameter, v in Eqs. 32 and 33. The nominal values of the parameters used were described in the above test cases. The output feedback controller however was designed using a ROM with $v = 0.35$ instead of using a nominal value of $v = 0.25$. The designed controller in Eq. 24 successfully stabilized the process and no significant difference was observed in the way it stabilizes the plant as compared to the above results of case 2. To further test the robustness of the approach, we computed the local ROM using the value of 90% for the energy criterion ($\varepsilon = 0.9$). Figures 14a, b present the temporal profile of L_2 norm and the Lyapunov function of the closed-loop system under the action of the designed controller in Eq. 24, respectively. We note that after the observed initial convergence the L_2 norm starts to increase at $t \approx 2$ as the local ROM (due to low dimensionality) failed to capture the new closed-loop trends. This is due to the small chosen value of the energy criterion ε. However, APOD detected these non-captured new trends and automatically increased the dimensionality of the local ROM at $t \approx 3$. Figure 14c presents this change in the dimensionality of the local ROM. Note that since the evolution of V in Figure 14b satisfied the hybrid stability requirements of Eq. 31 in lemma 1 it is, thus, implied that the process was always closed-loop stable. Subsequently, the controller designed using this local ROM (with increased dimensionality) stabilized the process at $x(z, t) = 0$. Note that ζ was set to be $\zeta = 1$ in the beginning of the simulation and it was not necessary to update its value during the process evolution. Thus, even though the error increased due to poorly chosen tunable parameter values, the proposed methodology was robust in stabilizing the process at the desired steady-state.

Conclusions

We presented a methodology for the efficient design of output feedback controllers for spatially distributed processes that are mathematically modeled by HDPDEs. This methodology which we coin Gappy APOD is specifically tailored to address important questions that arise when only partial information of the state profile is available. Initially, the partial states were reconstructed using gappy iteration procedure. These reconstructed measurements were then utilized for derivation and update of ROMs using APOD methodology. The efficient recursive ROM updates by APOD allowed us to use low-dimensional models while designing controllers, thus resulting in computational savings. The proposed methodology was illustrated on the Kuramoto-Sivashinsky equation, where the controller successfully stabilized the system at an open-loop unstable steady state.

Acknowledgments

Financial support from National Science Foundation, CAREER Award #CBET 06-44519 is gratefully acknowledged.

Literature Cited

1. Temam R. *Infinite-Dimensional Dynamical Systems in Mechanics and Physics*. New York: Springer-Verlag, 1988.
2. Balas MJ. Feedback control of linear diffusion processes. *Int J Control*. 1979;29:523–533.
3. Curtain RF, Glover K. *Balanced Realisations for Infinte-Dimensional Systems. Operator Theory and System*. Basel: Birkhauser, 1986.
4. Balas MJ. Nonlinear finite-dimensional control of a class of nonlinear distributed parameter systems using residual mode filters: a proof of local exponential stability. *J Math Anal Appl*. 1991;162:63–70.
5. Titi ES. On approximate inertial manifolds to the Navier-Stokes equations. *J Math Anal Appl*. 1990;149:540–557.
6. Christofides PD, Daoutidis P. Finite-dimensional control of parabolic PDE systems using approximate inertial manifolds. *J Math Anal Appl*. 1997;216:398–420.
7. El-Farra N, Armaou A, Christofides PD. Analysis and control of parabolic PDE systems with input constraints. *Automatica*. 2003;39:715–725.
8. Mahmood M, Mhaskar P. Safe-parking framework for fault-tolerant control of transport-reaction processes. *Ind Eng Chem Res*. 2010;49:4285–4296.
9. Christofides PD. *Nonlinear and Robust Control of PDE Systems*. New York: Birkhäuser, 2001.

10. Sirovich L. Turbulence and the dynamics of coherent structures: part I, II and III. *Q Appl Math*. 1987;45:561–590.
11. Holmes P, Lumley JL, Berkooz G. *Turbulence, Coherent Structures, Dynamical Systems and Symmetry*. New York: Cambridge University Press, 1996.
12. Graham MD, Kevrekidis IG. Alternative approaches to the Karhunen-Loève decomposition for model reduction and data analysis. *Comp Chem Eng*. 1996;20:495–506.
13. Rathinam M, Petzold LR. A new look at proper orthogonal decomposition. *SIAM J Numer Anal*. 2003;41:1893–1925.
14. Astrid P, Weiland S, Willcox K, Backx T. Missing point estimation in models described by proper orthogonal decomposition. *IEEE Trans Autom Contr*. 2008;53:2237–2251.
15. Shvartsman SY, Kevrekidis IG. Nonlinear model reduction for control of distributed systems: a computer-assisted study. *AIChE J*. 1998;44:1579–1595.
16. Demetriou MA, Smith RC. *Research Directions in Distributed Parameter Systems*. SIAM Frontiers in Applied Mathematics, Philadelphia: SIAM 2003.
17. Atwell JA, Borggaard JT, King BB. Reduced order controllers for Burger's equation with a nonlinear observer. *Int J Appl Math Comput Sci*. 2001;11:1311–1330.
18. Xu C, Ou Y, Schuster E. Sequential linear quadratic control of bilinear parabolic PDEs based on POD model reduction. *Automatica*. 2011;47:418–426.
19. Singler JR, Batten BA. Balanced POD Algorithm for robust control design for linear distributed parameter systems. In: *Proceedings of the American Control Conference*, Baltimore, MD, 2010:4881–4886.
20. Pitchaiah S, Armaou A. Output feedback control of distributed parameter systems using adaptive proper orthogonal decomposition. *Ind Eng Chem Res*. 2010;49:10496–10509.
21. Varshney A, Pitchaiah S, Armaou A. Feedback control of dissipative distributed parameter systems using adaptive model reduction. *AICHE J*. 2008;55:906–918.
22. Everson R, Sirovich L. The Karhunen Loève procedure for gappy data. *J Opt Soc Am*. 1995;12:1657–1664.
23. Thanh TB, Damodaram M, Willcox K. Aerodynamic data reconstruction and inverse design using proper orthogonal decomposition. *AIAA J*. 2004;42:1505–1516.
24. Venturi D, Karniadakis GM. Gappy data and reconstruction procedures for flow past a cylinder. *J Fluid Mech*. 2004;519:315–336.
25. El-Farra NH, Christofides PD. Robust inverse optimal control of nonlinear systems. *Int J Robust Nonlinear Control*. 2003;13:1371–1388.
26. Khalil HK. *Nonlinear Systems*, 3rd ed. New Jersey: Prentice Hall, 2002.
27. Declaro RA, Branicky MS, Pettersson S, Lennartson B. Perspectives and results on the stability and stabilizability of Hybrid systems. *Proc IEEE*. 2000;88:1069–1082.
28. Chang HC. Nonlinear waves on liquid film-surfaces-.I.Flooding in vertical tube. *Chem Eng Sci*. 1986;41:2463–2476.
29. Kevrekidis IG, Nicolaenko B, Scovel JC. Back in the saddle again: a computer assited study of the Kuramoto-Sivashinksy equation. *SIAM J Appl Math*. 1990;50:760–790.
30. Armaou A, Christofides PD. Dynamic optimization of dissipative PDE systems using nonlinear order reduction. *Chem Eng Sci*. 2002;57:5083–5114.

Manuscript received Oct. 26, 2011, and revision received May 4, 2012.